Supporting Information

Simultaneous on-site visual identification of norovirus GI and GII genogroups with point-of-care molecular lateral flow strip

Ziwen Zong[1], Xianzhuo Meng[1], Weiwei Li[2], Jianguo Xu[1], Junling Yu[2], Xinxin Wang[2], Peng Wang[2], Guodong Liu[3]， Yong Sun[2,*], Wei Chen[1,*]

[1]Engineering Research Center of Bio-process, MOE, School of Food and Biological Engineering, Hefei University of Technology, Hefei 230009, P. R. China

[2]Center of Disease Control and Prevention of Anhui Province, Hefei, 230009, China

[3]School of Chemistry and Chemical Engineering, Linyi University, Linyi, 276005, China

* Corresponding email: chenweishnu@163.com (W. C., ORCID: 0000-0003-3763-1183)

12 **Table S1.** The sequence and functionalization information of primer sets

Name	Primer	Sequence	Product size
NoV GI	GI-F	5’-FITC-CTGCCCGAATTYGTAAATGA-3’	330 bp
	GI-R	5’-Biotin-CCAACCCARCCATTRTACA-3’	
NoV GII	GII-F	5’-Dig-TGAGATTCTCAGATCTGAGCACGTGGGA-3’	132 bp
	GII-R	5’-FITC-ATTATTGACCTCTGGGACGAGGTTGGCT-3’	

13

14

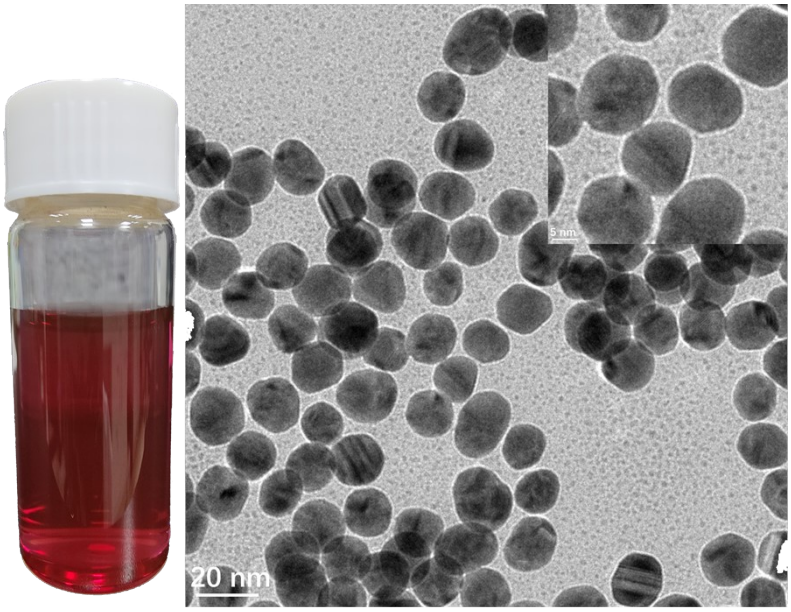

15

16 **Fig. S1** Characterization of AuNPs. AuNPs of wine red in a glass bottle, and TEM image (20 nm

17 and 5 nm) of AuNPs.

Optimization of experimental conditions of mPCR and LFS

To ensure efficient nucleic acid amplification, annealing and extension steps were performed at different temperatures. **Fig. S2A** and **Fig. S2B** demonstrate that amplification efficiency gradually increases with increasing annealing temperature, but is significantly inhibited beyond a certain point. Similarly, for extension temperatures, short fragment product extension becomes less favorable at higher temperatures (**Fig. S2C**, **S2D**). After combining these results with signal intensity of T lines (**Fig. S4A**, **S4B**), 54℃ was chosen as the optimal anneal temperature and 66℃ for extension. Different primer concentrations were used to investigate the effect on amplification efficiency. Increasing the NoV GI primer set slightly suppressed the amplification efficiency of NoV GII, while increasing the NoV GII primer set resulted in a gradual suppression of NoV GI (**Fig. S3A**, **S3C**). **Fig. S3B** and **Fig. S3D** showed the effect of different primer concentrations on the determination of results from the perspective of LFS visual detection. **Fig. S4C** and **Fig. S4D** showed the change of T-line signal intensity with primer concentration. Considering the need for simultaneous identification of GI and GII genogroups of norovirus, the optimal primer concentration for both was determined to be 240 nM. These conditions ensure that both genogroups can be adequately amplified with balanced competition between each other.

To ensure the consistency of amplification results with corresponding LFS visualization measurements, we have investigated various parameters that impact the performance of the LFS assay. These parameters include the amount of AuNP-FITC antibody conjugates present on the conjugation pad, the quantity of FITC antibody coupled to the surface of gold nanoparticles, as well as the concentrations of Digoxin antibody and SAV.

We conducted experiments to optimize several parameters affecting the performance of the LFS assay. Firstly, we investigated the impact of the amount of AuNP-FITC antibody conjugates on the conjugation pad, and found that the signal intensity of the two T lines increased with an increase in the amount of AuNP-FITC antibody conjugates, before eventually reaching saturation at 6 μL (**Fig. S5A**, **S6A**). Thus, we selected 6 μL as the optimal conjugates amount to ensure sufficient labeling of the two functional amplicons. Subsequently, we optimized the amount of FITC antibody coupled to the surface of gold nanoparticles to ensure a high target signal and well-suppressed background (**Fig. S5B**, **S6B**), and determined that 10 μL resulted in preventing the wastage of antibody. We selected 10 μL of FITC antibody for future assays. Finally, we studied the amounts of antibody sprayed on the test lines of LFS. While maintaining the SAV of T_1 line at 1.5 mg/mL, an elevation of Digoxin antibody concentration led to excessive adsorption of AuNP-FITC antibody conjugates on the T_2 line, resulting in weaker signal development intensity of the T_1 line (**Fig. S5C**, **S6C**). A Digoxin antibody concentration of 0.8 mg/mL led to a clear visual signal of the T_1 line, and thus this was selected for further experiments. Interestingly, as the amount of SAV increased, we observed that the signal intensity of the T_1 line gradually increased (**Fig. S5D**, **S6D**), but the expression of the T_2 line was not competitively suppressed. This may be due to the different antibody and affinity. We selected 2 mg/mL as the optimal concentration for SAV to ensure clear color rendering intensity of the T_1 line, while minimizing wastage.

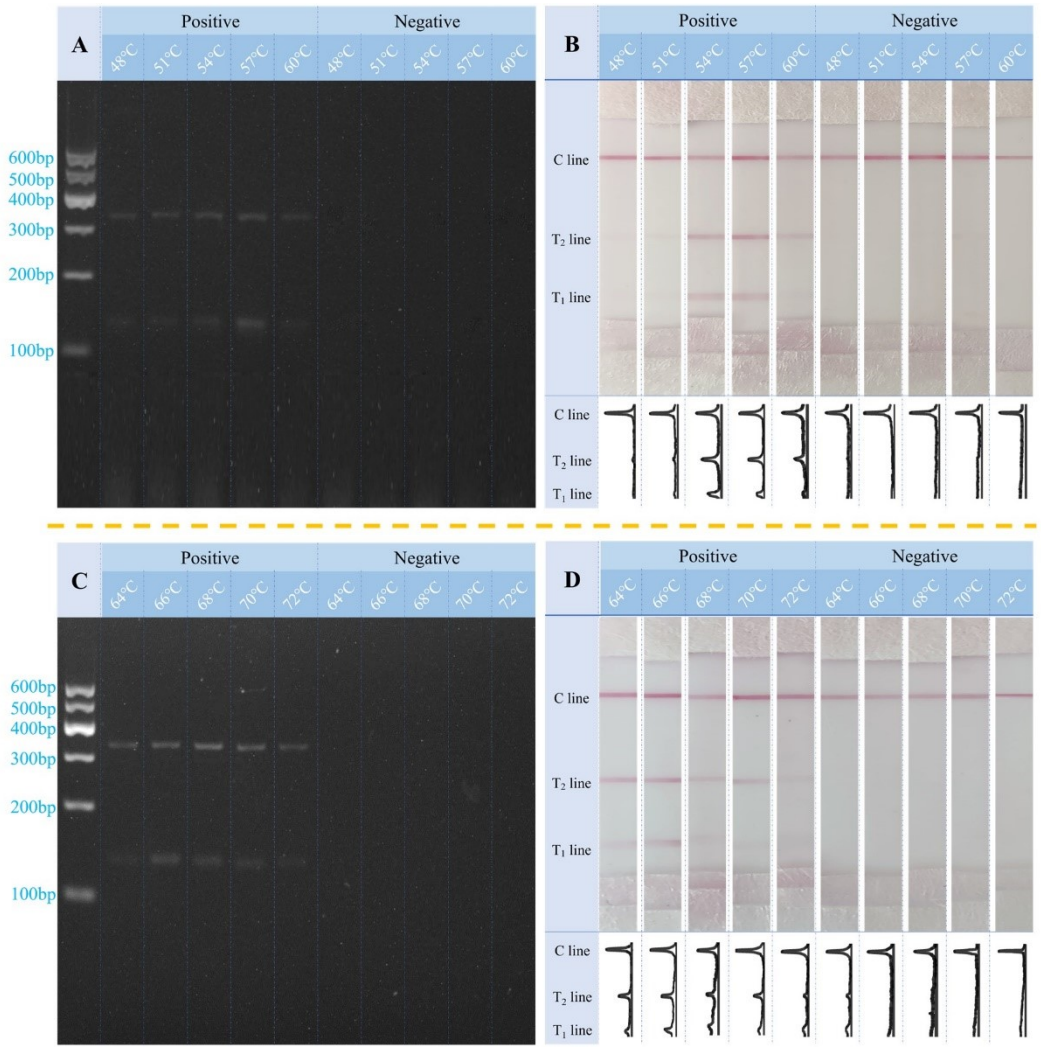

Fig. S2 Influence of the annealing temperature: Results of agarose gel electrophoresis (A) and LFS (B); Influence of the extension temperature: Results of agarose gel electrophoresis (C) and LFS (D).

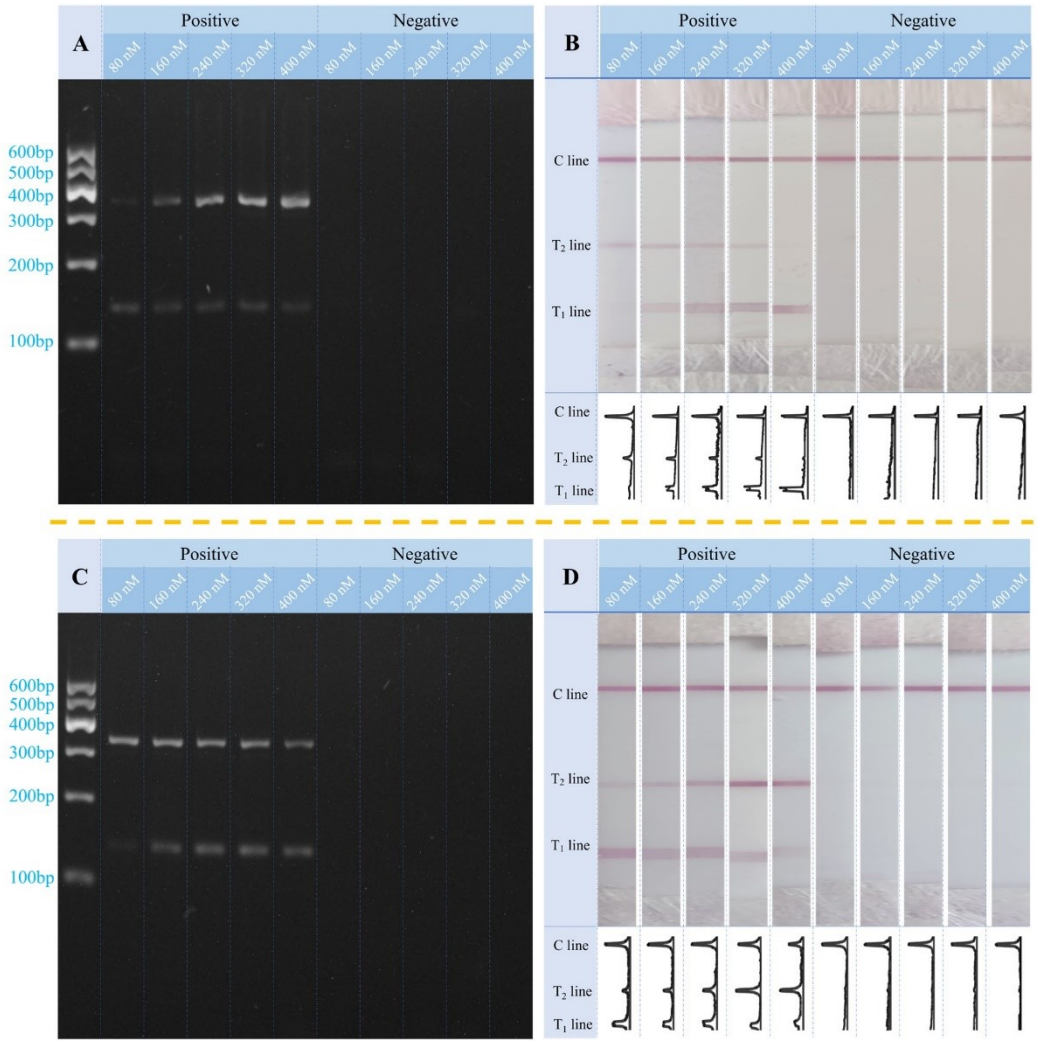

Fig. S3 Optimization of NoV GI/GII primer concentration: Results of agarose gel electrophoresis (A) and LFS (B) to increasing concentration of NoV GI primer; Results of agarose gel electrophoresis (C) and LFS (D) to increasing concentration of NoV GII primer.

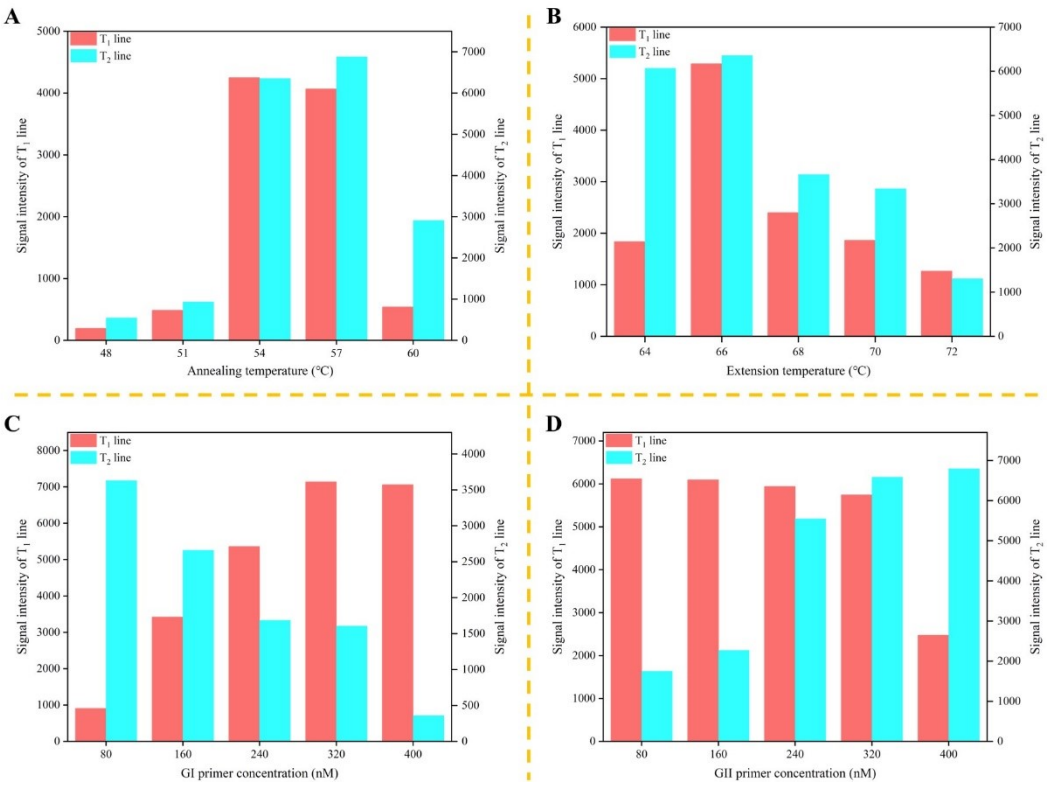

Fig. S4 The change of signal intensity with amplification conditions: (A) Annealing temperature; (B) Extension temperature; (C) Increasing concentration of NoV GI primer; (D) Increasing concentration of NoV GII primer.

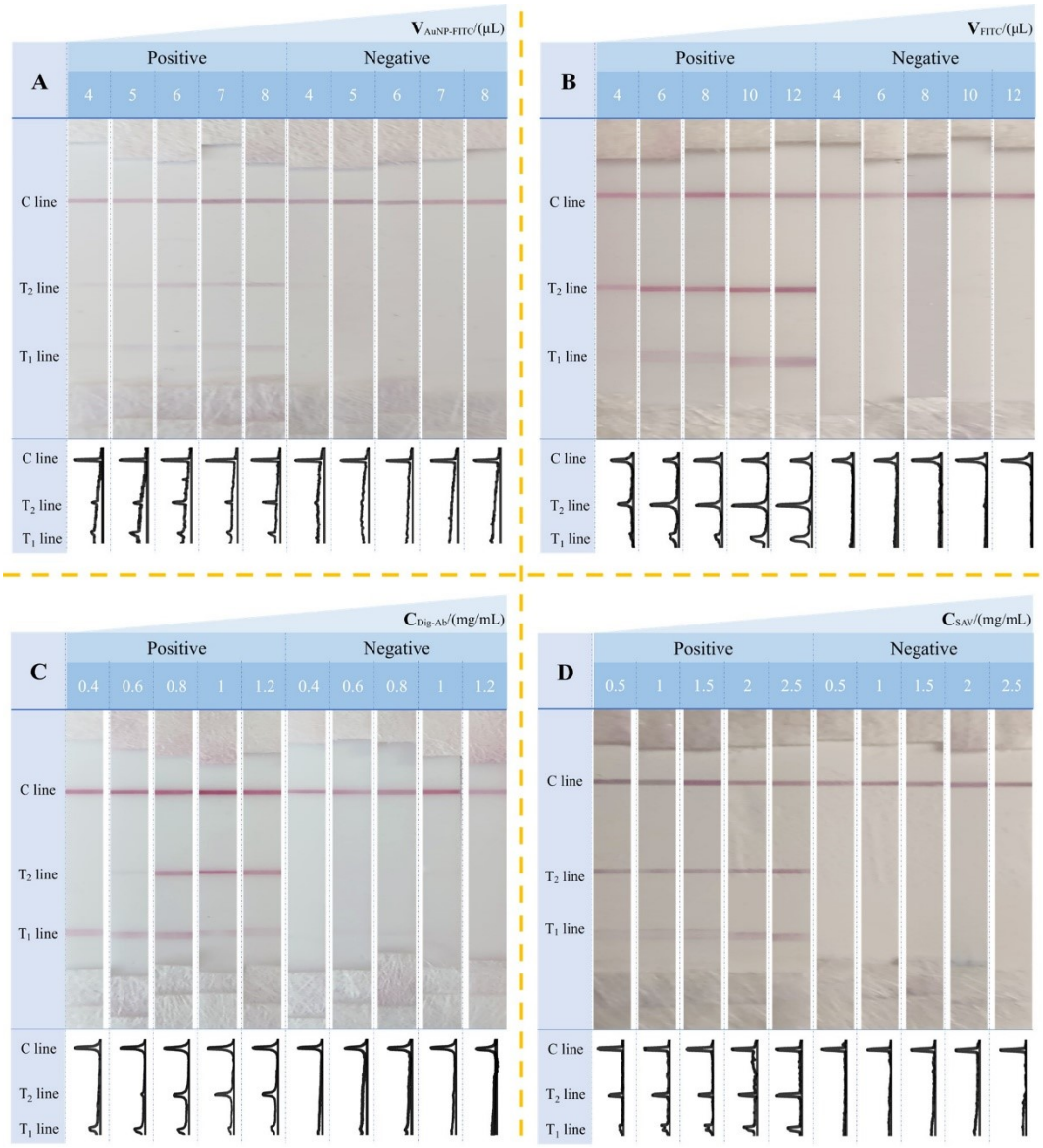

Fig. S5 Results of optimized LFS conditions: (A) Signal responses of LFS to increasing volume of AuNP-FITC antibody conjugates on the conjugation pad; (B) Signal responses of LFS to increasing volume of FITC antibody; (C) Signal responses of LFS to increasing concentration of Digoxin antibody (Dig-Ab) on the T_2 line; (D) Signal responses of LFS to increasing concentration of SAV on the T_1 line.

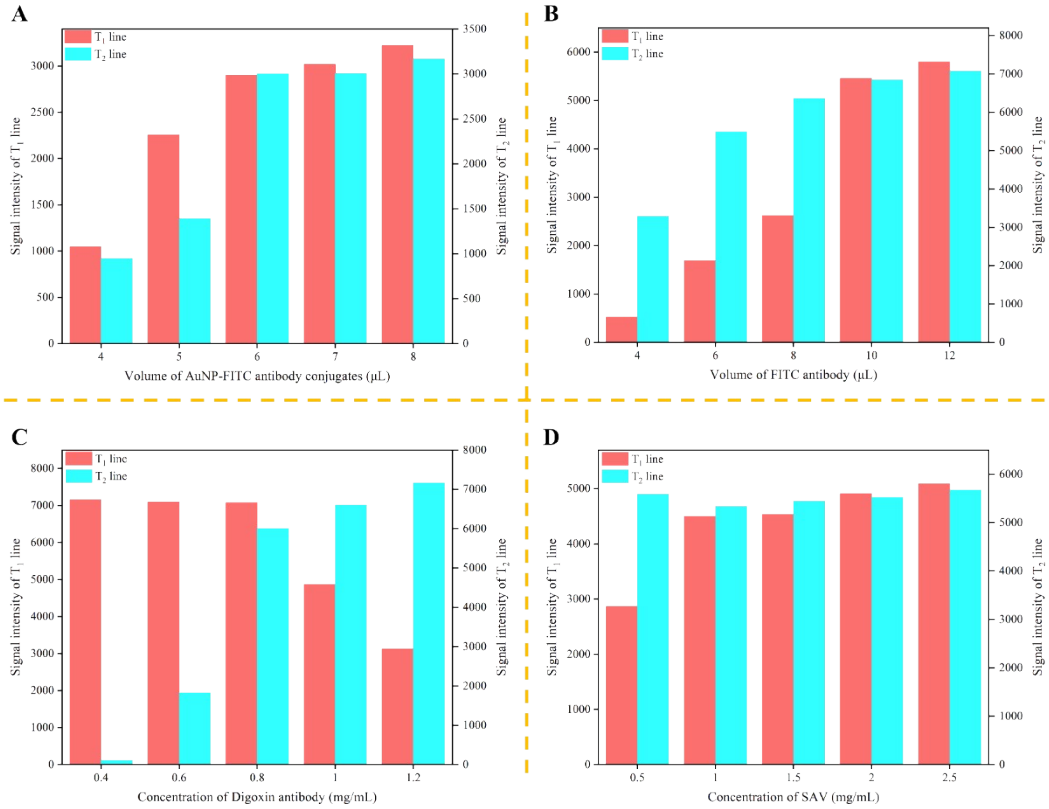

78

79 **Fig. S6** The change of signal intensity with optimized LFS conditions: (A) Increasing volume of

80 AuNP-FITC antibody conjugates on the conjugation pad; (B) Increasing volume of FITC antibody;

81 (C) Increasing concentration of Digoxin antibody (Dig-Ab) on the T2 line; (D) Increasing

82 concentration of SAV on the T_1 line.

83

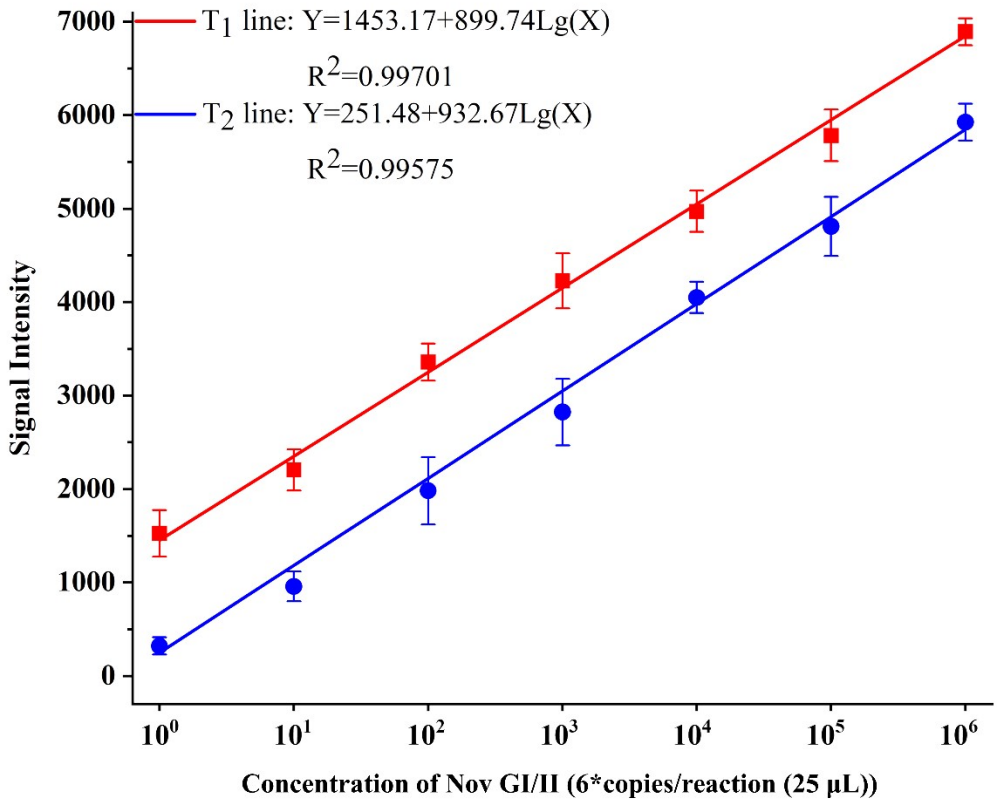

84

85 **Fig. S7** Quantitative analysis of mPCR-LFS for multiple testing of NoV GI and GII. From left to

86 right: 6×10^0, 6×10^1, 6×10^2, 6×10^3, 6×10^4, 6×10^5, 6×10^6 copies/reaction (25 μL).

87

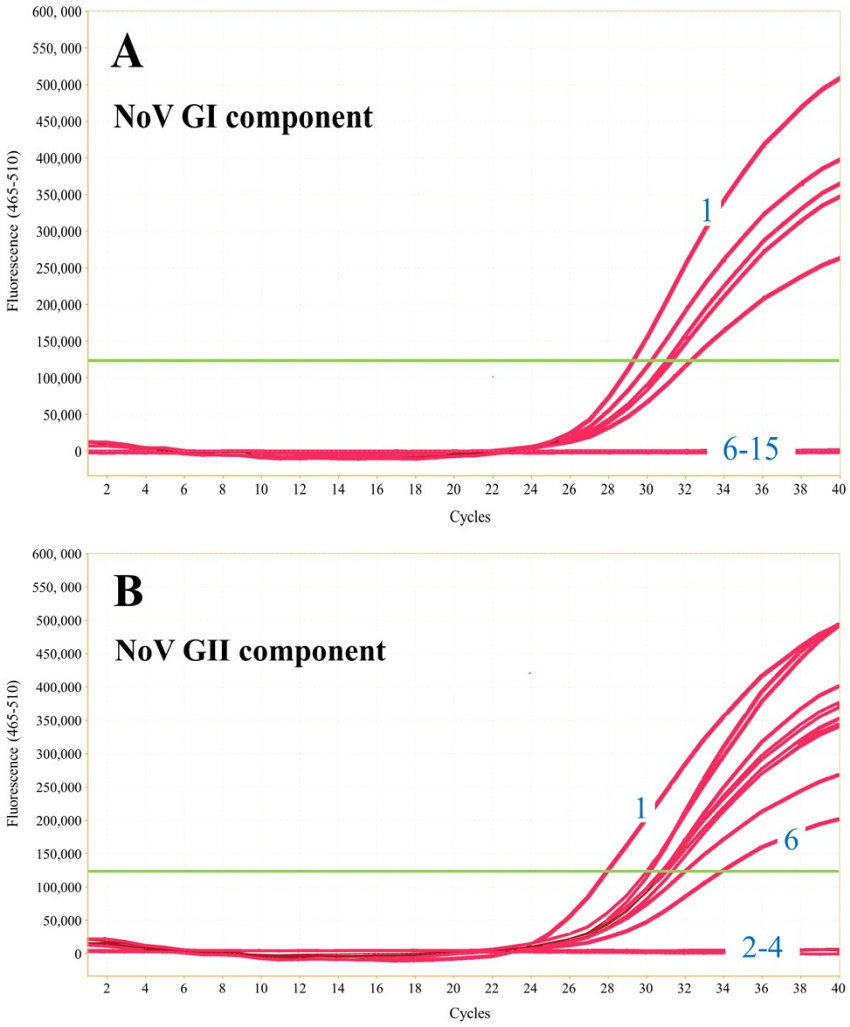

Fig. S8 The real-time PCR analysis results of the different components in all practical clinical samples. (A) Detection of NoV GI component in all clinical samples; (B) Detection of NoV GII components in all clinical samples.

Table S2 Comparison of recent reported methods for the detection of NoV GI/GII.

No.	Detection methods	Target	LOD	Reference
1	RT-LAMP	NoV GI and GII	10^2 and 10^3 copies/μL, NoV GI and GII	[1]
2	RT-LAMP	NoV GII	10^3 copies/μL	[2]
3	Split G-quadruplex	NoV GII	4 nM	[3]
4	Electrochemical sensor	NoV GII	100 pM	[4]
6	mPCR-LFS	NoV GI and GII	6 copies/reaction	This study

Reference

1. S. Fukuda, S. Takao, M. Kuwayama, Y. Shimazu and K. Miyazaki, *J. Clin Microbiol*, 2006, **44**, 1376-1381.
2. J. Luo, Z. Xu, K. Nie, X. Ding, L. Guan, J. Wang, Y. Xian, X. Wu and X. Ma, *Food. Environ. Virol.*, 2014, **6**, 196-201.
3. K. Nakatsuka, H. Shigeto, A. Kuroda and H. Funabashi, *Biosens. Bioelectron.*, 2015, **74**, 222-226.
4. R. Chand and S. Neethirajan, *Biosens. Bioelectron.*, 2017, **98**, 47-53.